

# Connections between reflected entropies and hyperbolic string vertices

Peng Wang<sup>a</sup>, Houwen Wu<sup>a,b</sup> and Haitang Yang<sup>a</sup>

<sup>a</sup>*College of Physics  
Sichuan University  
Chengdu, 610065, China*

<sup>b</sup>*DAMTP, Centre for Mathematical Sciences  
University of Cambridge  
Cambridge, CB3 0WA, UK*

pengw@scu.edu.cn, hw598@damtp.cam.ac.uk, hyanga@scu.edu.cn

## Abstract

In this paper, we establish connections between the reflected entropies of multipartite mixed states in  $\text{CFT}_2$  and hyperbolic string vertices of closed string field theory (CSFT). We show that the reflected surfaces, which are bulk duals of the reflected entropies, share the same Riemann surfaces with the hyperbolic string vertices. This observation enables us to build quantitative relations between the reflected entropies and hyperbolic string vertices. We illustrate the connections with several examples. Consequently, we propose that spacetime structure could be directly generated from the hyperbolic string vertices. The advantage of the hyperbolic string vertices approach is that we have a dynamical equation, the Batalin-Vilkoviski master equation, to control the generating process.

# Contents

|          |  |           |
|----------|--|-----------|
| <b>1</b> | <b>Introduction</b>  | <b>2</b>  |
| <b>2</b> | <b>Preliminaries</b>   | <b>4</b>  |
| 2.1      | Hyperbolic string vertices in CSFT . . . . .                           | 4         |
| 2.2      | Canonical purification and reflected entropy . . . . .                 | 7         |
| <b>3</b> | <b>Connections between string vertices and reflected entropies</b>     | <b>11</b> |
| 3.1      | Construct reflected surfaces from string vertices . . . . .            | 13        |
| 3.2      | Remove the equal length restriction . . . . .                          | 18        |
| <b>4</b> | <b>Preliminary evidence</b>  | <b>19</b> |
| <b>5</b> | <b>Hyperbolic closed string vertices as spacetime building blocks?</b> | <b>22</b> |
| <b>6</b> | <b>Conclusion and discussions</b>                                      | <b>24</b> |

## 1 Introduction

It is well known that closed string field theory (CSFT) has two equivalent descriptions [1]. The first one uses a conformal field theory to represent a string background. The second one adopts background independent string vertices [2,3], and it therefore attracted much more attention. In early works [4], Zwiebach demonstrated that, if all consistent string vertices and their corresponding suitable conformal field theory are known, bosonic closed string field theory can be constructed. These consistent string vertices are required to satisfy a geometric version of the Batalin-Vilkoviski (BV) master equation, i.e. geometric master equation. Therefore, one main task in CSFT is to seek all the consistent string vertices which exactly solve the geometric master equation.

The development of the string vertices has mainly experienced three stages. The first approach is to consider Riemann surfaces endowed with a minimal area metric, which enables a decomposition of a moduli space [4,5]. It is then simple to specify the string vertices respecting the BV equation. However, this approach only works perfectly for genus zero surfaces. For higher genus ( $g \geq 1$ ) surfaces, the existence of the minimal area metric has no proof.

As an alternative proposal, Moosavian and Pius used the hyperbolic surfaces to construct the string vertices [6,7]. The proof of existence is no question, but the BV equation is not exactly solved. To satisfy the BV equation, higher order corrections are needed and their existence is unknown.

In a recent work [8], Costello and Zwiebach made a simple but brilliant improvement on the Moosavian-Pius's approach, that is, replace the horocycle, which is the boundary of the coordinate disks around the punctures in

the Moosavian-Pius surface, by geodesics of length  $0 < L \leq 2\text{arcsinh}(1)$ . The consistent string vertices, called as hyperbolic string vertices, are those whose systole<sup>1</sup> is not less than  $L$ . These hyperbolic string vertices solve the BV equation exactly. Cho soon generalized this method to construct the open-closed string vertices [9].

The minimal area approach and Moosavian-Pius construction turn out to be limits of the hyperbolic string vertices. As verified in [10], the simplest hyperbolic 3-string vertex (Y-piece) with boundary length  $L$ , when  $L \rightarrow \infty$ , reduces to the minimal area 3-string vertex. On the other hand, as  $L \rightarrow 0$ , it becomes the naive three-string vertex [6, 7] or Kleinian vertex [11].

Another background ingredient needed in this article is the reflected entropy, which is a generalization of the entanglement entropy to the mixed state systems. The entanglement entropy (EE) measures the correlation between subsystems of a pure system. It is one of the most distinct features of quantum systems. Dividing a pure system into two subsystems:  $A$  and  $B$ , the total Hilbert space is accordingly decomposed as  $\mathcal{H} = \mathcal{H}_A \otimes \mathcal{H}_B$ . Tracing out degrees of freedom of the region  $B$ , one obtains a reduced density matrix of the region  $A$ :  $\rho_A = \text{Tr}_{\mathcal{H}_B} \rho$ . The entanglement entropy of the region  $A$  is evaluated by the von Neumann entropy  $S_A = -\text{Tr}_{\mathcal{H}_A} (\rho_A \log \rho_A)$ . It is clear that  $S_A = S_B$ .

Motivated by AdS/CFT correspondence and Bekenstein-Hawking entropy of black holes, Ryu and Takayanagi (RT) proposed that the minimal surface area ending on the  $d$  dimensional boundary of  $\text{AdS}_{d+1}$  corresponds to the entanglement entropy of  $\text{CFT}_d$  living on the boundary of  $\text{AdS}_{d+1}$  [12]. For  $d = 2$ , the minimal surfaces are geodesics and the RT formula has been verified extensively.

However, the entanglement entropy is ill-defined for mixed states. One obvious feature is that the entanglement entropy of mixed states is always nonzero whether they are entangled or not. One method to solve this problem is to purify the mixed state and then introduce the entanglement of purification  $E_P$ , whose bulk dual is conjectured as the area of entanglement wedge cross-section  $E_W$ , namely  $E_P = E_W$  [13]. Usually, calculating  $E_P$  is very difficult since it involves minimization over all possible purifications. For this reason, in [14], a much simpler alternative has been proposed, namely the canonical purification, which defines the reflected entropy  $S_R$ . The bulk interpretation of the canonical purification is developed in [15]. The bulk dual of the reflected entropy is called reflected surface, also denoted as  $S_R$  if not confused. For a bipartite system, it turns out  $S_R(A : B) = 2E_W(A : B)$ . Discussions on the multipartite reflected entropy and its bulk interpretation can be found in refs. [16, 17].

Careful studies find that both the hyperbolic string vertices and the reflected surfaces are hyperbolic surfaces bounded by geodesics. They furthermore share very similar construction procedures. In addition, theorems in hyperbolic geometry impose strict constraints on the structure of surfaces. We are therefore motivated to establish connections between the hyperbolic string vertices and the bulk geometries of multipartite canonical purification.

There are two obstacles to build the connections. The boundary lengths of the string vertices are constrained to be the same while those of reflected surfaces are allowed to be different. We will show that this problem can be solved by constructing procedures. A more serious problem is that the boundary lengths of the (quantum) string vertices have an upper bound  $L \leq L_* = 2\text{arcsinh } 1$ , but those of reflected surfaces have a lower bound  $S_R > 2L_*$ . It turns out this sharp contradiction is solved magically by intrinsic properties of hyperbolic geometry.

---

<sup>1</sup>The systole  $\text{syst}[\Sigma]$  of a surface  $\Sigma$  is defined as the length of the shortest non-contractible closed geodesic which is not a boundary component.

Since it is widely believed that the spacetime structure could be generated by the entanglement entropy through the dual surfaces, once the connections between the hyperbolic string vertices and reflected entropies/surfaces are established, we are led to ask if the spacetime could directly emerge from the hyperbolic string vertices. A great advantage of the hyperbolic string vertex approach is that the generating process is completely controlled by the BV master equation.

This paper is organized as follows. In section 2, we provide background reviews for hyperbolic string vertices of CSFT and canonical purification of CFT. In section 3, we establish the connections between the closed string vertices and the bulk geometries of canonical purification. Several examples are supplied to illustrate the connections. In Section 4, we provide a preliminary evidence to reinforce the connections. In Section 5, we argue that spacetime can be built by the string vertices. The last section includes the conclusion and discussions.

## 2 Preliminaries

In this section, we briefly review the two ingredients on which our results are based. We first show the construction of the simplest string vertex  $\mathcal{V}_{0,3}(L)$  in detail and give some theorems needed in the rest of this work. Subsection 2.2 is devoted to a simple introduction to the reflected entropy and the dual reflected surfaces.

### 2.1 Hyperbolic string vertices in CSFT

In closed string field theory, off-shell amplitudes are defined by a set of string vertices  $\mathcal{V}_{g,n}$ , which are subsets of *moduli spaces*  $\hat{\mathcal{P}}_{g,n}$  of compact Riemann surfaces of genus  $g$  and  $n$  marked points, with local coordinates defined around those marked points up to phases. These vertices have negative Euler numbers  $2g + n - 2 > 0$  and thus admit hyperbolic metrics of constant negative Gaussian curvature. To get a consistent quantum theory, these string vertices must satisfy the Batalin-Vilkoviski (BV) master equation,

$$\partial\mathcal{V} + \hbar\Delta\mathcal{V} + \frac{1}{2}\{\mathcal{V}, \mathcal{V}\} = 0, \quad (2.1)$$

where

$$\mathcal{V} = \sum_{g,n} \hbar^g \mathcal{V}_{g,n}, \quad \text{with} \quad \begin{cases} n \geq 3, & \text{for } g = 0, \\ n \geq 1, & \text{for } g = 1, \\ n \geq 0, & \text{for } g \geq 2. \end{cases} \quad (2.2)$$

In eq. (2.1), geometrically,  $\partial$  indicates the boundary of a moduli space.  $\Delta$  denotes removing the disks of two marked points on one Riemann surface, and then twist-sewing the boundaries of these two disks.  $\{ , \}$  stands for removing two disks on two input Riemann surfaces respectively, and then twist-sewing them together [2, 3]. In a recent remarkable work [8], Costello and Zwiebach proved that the closed string vertices can be simply and elegantly constructed by using the hyperbolic geometry. For the purpose to show the connections with the reflected surfaces plainly, we demonstrate the construction of the fundamental building block  $\mathcal{V}_{0,3}(L)$  from the very beginning, in four steps:

### Step one:

The first step is to prepare a right-angled hexagon with side lengths  $L/2, \vartheta, L/2, \vartheta, L/2, \vartheta$  on a hyperbolic surface. Refer to Fig. (1), the construction is to begin with a Poincare disk and plot three boundary-anchored equal length geodesics (in red color)  $\gamma_a = \gamma_b = \gamma_c$  ( $a = b = c$  and  $A = B = C$  on the boundary). Then, the hexagon is uniquely fixed by the following theorem:

**Theorem 1** (Ultra-parallel theorem, [20] Theorem 1.1.6): In the Poincare disk, if  $\gamma_a$  and  $\gamma_c$  are disjoint geodesics with positive distance, then there exists a unique (blue colored) geodesic perpendicular to them.

The lengths of the blue geodesics are denoted as  $L/2$ , which are of course the shortest lines connecting  $\gamma_i$ . The lengths of the other three red geodesics of the hexagon are  $\vartheta$ . Trigonometry of hyperbolic geometry [20] (Theorem 2.4.1) gives

$$\cosh \vartheta = \frac{\cosh(L/2)}{\cosh(L/2) - 1} \quad (2.3)$$

Therefore, the hexagon is enclosed by the blue and red geodesics.

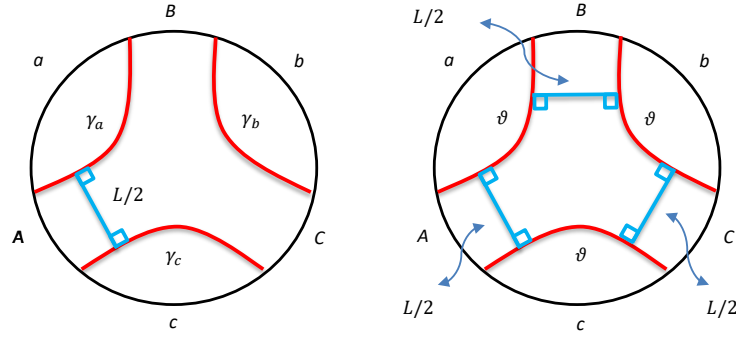


Figure 1: The constructed right-angled hexagon is bounded by the blue and red geodesics.

### Step two:

Gluing two copies of this hexagon along the red geodesics  $\vartheta$ , we get an  $\tilde{\mathcal{V}}_{0,3}(L)$ , called a Y-piece whose three geodesic boundaries having lengths  $(L/2) \times 2 = L$ , as depicted in Fig. (2).

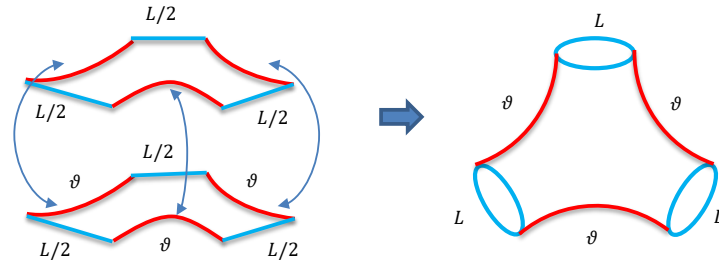


Figure 2: Glue two right-angled hexagons to obtain a Y-piece.

The systole  $\text{sys}[\Sigma]$  of a surface  $\Sigma$  is defined as the length of the shortest non-contractible closed geodesic which is not a boundary component. The construction itself guarantees  $\text{sys}[\tilde{\mathcal{V}}_{0,3}(L)] \geq L$ .

### Step three:

The third step is to graft flat semi-infinite cylinders of circumference  $L$  to the geodesic boundaries of  $\tilde{\mathcal{V}}_{0,3}(L)$ , to obtain the string vertices  $\mathcal{V}_{0,3}(L)$ , see Fig. (3).

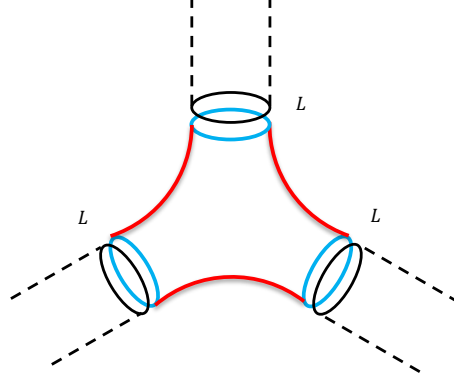


Figure 3:  $\tilde{\mathcal{V}}_{0,3}(L) \rightarrow \mathcal{V}_{0,3}(L)$  by grafting semi-infinite cylinders.

The flat semi-infinite cylinders can be conformally mapped to the marked points with local coordinates. Moreover, the cylinders can be seen as the Feynman propagators which are used to connect different string vertices. Higher order string vertices  $\mathcal{V}_{g,n}(L)$  are built by gluing Y-piece  $\tilde{\mathcal{V}}_{0,3}(L)$  along the geodesic boundaries to form  $\tilde{\mathcal{V}}_{g,n}(L)$ , and then grafting flat semi-infinite cylinders to the boundaries of  $\tilde{\mathcal{V}}_{g,n}(L)$ .

### Step four

To solve the geometric master equation (2.1), the boundary geodesic length  $L$  of  $\mathcal{V}_{g,n}(L)$  is required to satisfy some constraints based on the Collar theorem.

**Theorem 2** (Collar theorem, [20] Theorem 4.1.1): Let  $\sigma_i$  be simple closed geodesics on a hyperbolic surface  $S$ , the collars

$$\mathcal{C}(\sigma_i) = \left\{ p \in S \mid d(p, \sigma_i) \leq \frac{\omega_i}{2} \right\}, \quad (2.4)$$

of widths  $\omega_i$

$$\sinh\left(\frac{1}{2}\omega_i\right) \sinh\left(\frac{1}{2}L(\sigma_i)\right) = 1, \quad (2.5)$$

are pairwise disjoint. We illustrate the simplest example  $\tilde{\mathcal{V}}_{0,3}(L)$  in Fig. (4).

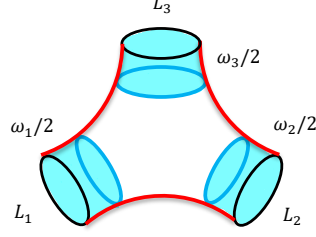


Figure 4: Collars respecting eq. (2.5) are pairwise disjoint.

A critical geodesic length  $L_*$  is defined as

$$\omega_* = L_* = 2 \operatorname{arcsinh}(1) = 2 \log(1 + \sqrt{2}) = \log(3 + 2\sqrt{2}). \quad (2.6)$$

A very useful proposition can be proved with the Collar theorem:

**Proposition 3** ([20] Proposition 4.1.2): Let  $\sigma, \delta$  be closed geodesics on a hyperbolic surface which intersect each other transversally, and assume  $\sigma$  is simple. Then

$$\sinh\left(\frac{\sigma}{2}\right) \sinh\left(\frac{\delta}{2}\right) > 1. \quad (2.7)$$

An immediate conclusion is that a simple geodesic of length  $L \leq L_*$  cannot intersect another geodesic of length  $L' \leq L_*$ . Based on these conclusions, in [8], Costello and Zwiebach proved:

1. The sets  $\mathcal{V}(L) = \sum_{n \geq 3} \mathcal{V}_{0,n}(L)$  whose boundary length is  $L > 0$  and  $\operatorname{sys}[\mathcal{V}(L)] \geq L$ , solve the classical geometric master equation ( $\hbar \rightarrow 0$  in (2.1)).
2. The sets  $\mathcal{V}(L) = \sum_{g,n} \mathcal{V}_{g,n}(L)$  whose boundary length is  $L \leq L_*$  and  $\operatorname{sys}[\mathcal{V}(L)] \geq L$ , solve the quantum geometric master equation (2.1).

Note that as Costello and Zwiebach demonstrated, for  $0 < L \leq L_*$ , the operation  $\Delta$  and  $\{, \}$  in the BV equation (2.1) maintain the systole of  $\tilde{\mathcal{V}}_{g,n}(L)$ . When constructing  $\tilde{\mathcal{V}}_{g,n}(L)$  from  $\tilde{\mathcal{V}}_{0,3}(L \leq L_*)$ , the systole does not change according to Proposition 3.

## 2.2 Canonical purification and reflected entropy

In this subsection, we provide a brief introduction to the reflected entropy and its bulk dual, namely reflected surfaces. Some recent progresses refer to [21].

Our discussion starts with the entanglement entropy of a pure state in  $\text{CFT}_2$ . Considering a quantum pure system  $|\psi\rangle$  which is divided into two parts  $A$  and  $B$ , the total Hilbert space is  $\mathcal{H} = \mathcal{H}_A \otimes \mathcal{H}_B$ . The reduced density matrix of the subsystem  $A$  is defined as  $\rho_A = \operatorname{Tr}_{\mathcal{H}_B} |\psi\rangle\langle\psi|$ . The entanglement entropy of the region  $A$  is given by the von Neumann entropy:

$$S_{EE}(A) = -\operatorname{Tr}_{\mathcal{H}_A} (\rho_A \log \rho_A). \quad (2.8)$$

It is clear that  $S_{EE}(A) = S_{EE}(B)$ .

Ryu and Takayanagi (RT) [12] realized that this entanglement entropy possesses a bulk interpretation. As illustrated in Fig. (5) for  $\text{AdS}_3/\text{CFT}_2$ , the bulk dual of the entanglement entropy is the area of the codimension-2 minimal surface  $\gamma_A$  (green line, geodesics for  $d = 2$ ) satisfying:  $\partial A = \partial \gamma_A$  and  $\gamma_A$  is homologous to  $A$ :

$$S_{EE}(A) = \frac{\text{Area}(\gamma_A)}{4G_N^{(3)}}, \quad (2.9)$$

where  $G_N^{(3)}$  is the 3-dimensional Newton constant. We will set  $4G_N^{(3)} = 1$  for simplicity in the following discussions.

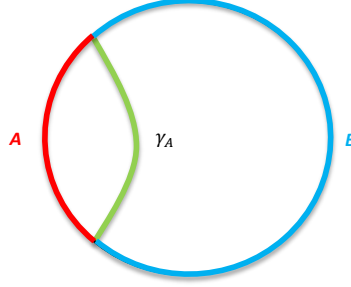


Figure 5: The entanglement entropy  $S_{EE}(A)$  can be evaluated by the length of geodesic  $\gamma_A$  (green line).

However, the entanglement entropy fails if the concerned state  $\rho_{AB}$  is a mixed state. The concept of entanglement of purification is thus introduced [23] to measure the entanglement of mixed states. We focus on bipartite mixed states here.

Suppose there is a mixed state  $\rho_{AB} = \sum_i p_i |i\rangle_{AB} \langle i|_{AB}$ , organized in terms of an orthonormal basis. By enlarging the Hilbert space from  $\mathcal{H}_A \otimes \mathcal{H}_B$  to  $\mathcal{H}_A \otimes \mathcal{H}_B \otimes \mathcal{H}'_A \otimes \mathcal{H}'_B$ , the mixed state  $\rho_{AB}$  is purified to a pure state  $|\sqrt{\rho_{AB}}\rangle_{AA'BB'} = \sum_i \sqrt{p_i} |i\rangle_{AB} \otimes |i\rangle_{A'B'}$ . It should be noted that the purification is far from unique. Then the entanglement of purification is defined as the von Neumann entropy between  $A \cup A'$  and  $B \cup B'$ :  $E_P(\rho_{AB}) = \min_{|\psi\rangle_{AA'BB'}} S_{EE}(A \cup A')$ , minimizing over all possible purifications.

The bulk interpretation of  $E_P$  is shown in Fig. (6). In this figure, the subsystems  $A$  and  $B$  are no longer complementary on the boundary. The procedure of purification provides the bulk geodesic regions  $A'$  and  $B'$ . Then the new subsystems  $A \cup A'$  and  $B \cup B'$  become complementary again. The entanglement wedge cross-section (EWCS)  $E_W$ , the green line in Fig. (6), is defined by minimizing the RT surface of  $A \cup A'$  and  $B \cup B'$  over  $A'$  and  $B'$ . It is conjectured that [13]:

$$E_P(\rho_{AB}) = E_W(A : B). \quad (2.10)$$

This is a generalization of the pure state situation. If  $\rho_{AB}$  is a pure state, one has  $E_P(\rho_{AB}) = E_W(A : B) = S_{EE}(A) = S_{EE}(B)$ .



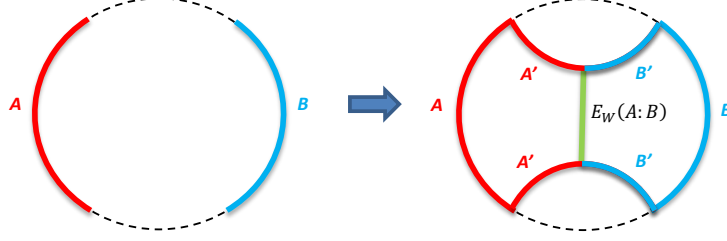


Figure 6: Purification of mixed states. The green line is the entanglement wedge cross-section  $E_W$ .

However, the entanglement of purification  $E_P(\rho_{AB})$  is difficult to calculate since it involves minimization over all possible purifications. For this reason, in [14], a much simpler alternative has been proposed, namely the reflected entropy  $S_R$ .

Instead of minimizing over all possible purifications, the reflected entropy simply selects an identical copy of the original mixed state as the purification, which is called canonical purification. Denoting the copied state as  $A^*B^*$ , the purified state and the reflected entropy are

$$|\sqrt{\rho_{AB}}\rangle_{AA^*BB^*} = \sum_i \sqrt{p_i} |i\rangle_{AB} \otimes |i\rangle_{A^*B^*}, \quad S_R(A:B) = S(AA^*)_{\sqrt{\rho_{AB}}} = -\text{Tr} \rho_{AA^*} \log \rho_{AA^*}, \quad (2.11)$$

where  $\rho_{AA^*} = \text{Tr}_{BB^*} |\sqrt{\rho_{AB}}\rangle\langle\sqrt{\rho_{AB}}|$ . If  $A \cup B$  is a pure state, the reflected entropy  $S_R(A:B)$  reduces to a double of the ordinary entanglement entropy  $S_R(A:B) = 2S_{EE}(A) = 2S_{EE}(B)$ .

The bulk dual of the reflected entropy is called reflected surface, which is also denoted as  $S_R(A:B)$ . For a bipartite mixed state  $(A, B, c, c')$ , as illustrated in Fig. (7), we first prepare a CPT copy  $(A^*, B^*, c, c')$ . The red curves  $\gamma_c$  and  $\gamma_{c'}$  are geodesics anchored on  $\partial c$  and  $\partial c'$  respectively. The reflected surface  $S_R(A:B)$  (green curve) is obtained by gluing two surfaces along  $\gamma_c$  and  $\gamma_{c'}$ . By definition, the reflected surface is a *closed simple geodesic* [14, 15] and one thus has

$$S_R(A:B) = 2E_W(A:B), \quad (2.12)$$

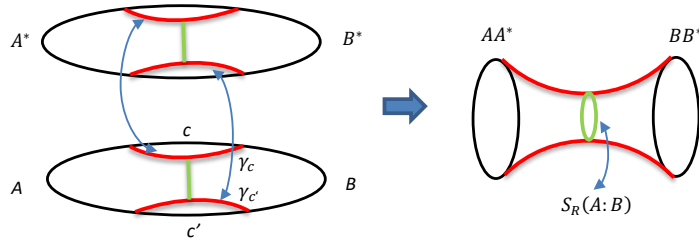


Figure 7: The surface  $(A^*, B^*, c, c')$  is a CPT copy of the original surface  $(A, B, c, c')$ .  $\gamma_c$  and  $\gamma_{c'}$  are geodesics anchored on  $\partial c$  and  $\partial c'$  respectively. The reflected surface  $S_R(A:B)$  is a closed simple geodesic, obtained by gluing along  $\gamma_c$  and  $\gamma_{c'}$ .

These constructions can be generalized to multipartite mixed states [16, 17]. The canonical purification of a tripartite mixed state is dual to gluing two copies of tripartitoned entanglement wedge along three red geodesics in the bulk, see Fig. (8).

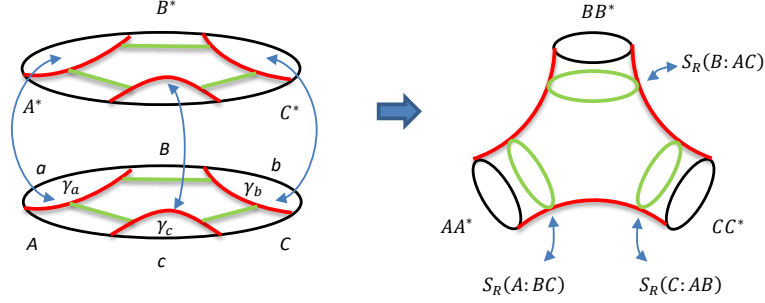


Figure 8: Bulk interpretation for tripartite canonical purification.

The lengths of green simple closed geodesics (reflected surfaces) are reflected entropies for bipartitions  $(A : BC)$ ,  $(B : AC)$  and  $(C : AB)$  in the boundary theory [17]:

$$\begin{aligned} S_R(A : BC) &= S(AA^* : BB^*CC^*)_{\sqrt{\rho_{ABC}}}, \\ S_R(B : AC) &= S(BB^* : AA^*CC^*)_{\sqrt{\rho_{ABC}}}, \\ S_R(C : AB) &= S(CC^* : AA^*BB^*)_{\sqrt{\rho_{ABC}}}. \end{aligned} \quad (2.13)$$

### Lower bound of $S_R$

Unlike the boundary of hyperbolic string vertices, whose lengths have an upper limit  $L \leq L_*$ , the length of a reflected surface  $S_R$  has a lower bound. This bound comes from the definition of the entanglement wedge cross section:

$$E_W(A : B) \geq \frac{1}{2} I(A : B), \quad (2.14)$$

where  $I(A : B) = S(\rho_A) + S(\rho_B) - S(\rho_{AB})$  is the mutual information. When  $A$  and  $B$  are distant, the mutual information  $I(A : B)$  vanishes [24], and therefore the corresponding bulk entanglement wedge becomes disconnected, namely  $E_W(A : B) = 0$ , see Fig. (9). In other words, the reflected entropy or entanglement wedge cross section does not always exist. There is a phase transition point between the connected and disconnected entanglement wedges.

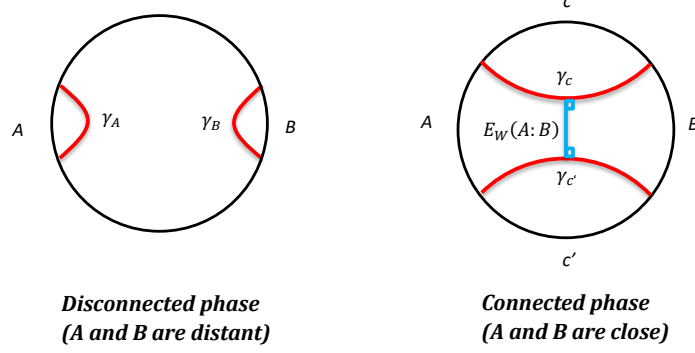


Figure 9: Phase transition between disconnected and connected phases.

The lower bound of  $S_R(A : B)$  and  $I(A : B)$  can be obtained either from CFT or geodesics in AdS (below eq. (21) in ref. [13] and below eq. (4.40) in ref. [14]). We simply present their results here. Suppose there are two regions  $A = [a_1, a_2]$  and  $B = [b_1, b_2]$ , where  $a_1 < a_2 < b_1 < b_2$ , the entanglement wedge cross section and the mutual information are given by

$$\begin{aligned} E_W(A : B) &= \log \left( 1 + 2z + 2\sqrt{z(z+1)} \right), \\ \frac{1}{2}I(A : B) &= \log z, \end{aligned} \quad (2.15)$$

where we set  $R = 4G_N = 1$  and  $z \geq 0$  is the cross ratio,

$$z = \frac{(a_2 - a_1)(b_2 - b_1)}{(b_1 - a_2)(b_2 - a_1)}. \quad (2.16)$$

From eq. (2.15),  $I(A : B)$  is truncated at  $z = 1$ . Therefore, at this value,  $E_W(A : B)$  reaches a lower bound,

$$E_W(A : B) > \log \left( 3 + 2\sqrt{2} \right). \quad (2.17)$$

Then, it is ready to get

$$S_R(A : B) = 2E_W(A : B) > 2\log \left( 3 + 2\sqrt{2} \right) = 2L_*, \quad (2.18)$$

which indicates that when the length of the green geodesic  $S_R(A : B)$  approaches  $2L_*$  in Fig. (7), the entanglement wedge, which is enclosed by the red geodesics, abruptly disappears and  $S_R(A : B)$  becomes zero. In addition, the tripartite entanglement wedge also requires the three bipartite reflected entropies satisfying  $S_R(A : BC)$ ,  $S_R(B : AC)$  and  $S_R(C : AB) \geq 2L_*$ .

### 3 Connections between string vertices and reflected entropies

We now see that both the boundaries of string vertices and reflected surfaces are simple closed geodesics in hyperbolic surfaces. According to Theorem 1, there is a unique geodesic perpendicular to two ultra-parallel

geodesics. We also have:

**Theorem 4** ([20] Theorem 3.1.7): Given any three positive numbers  $l_a, l_b, l_c$ , there exists a unique Y-piece whose boundary geodesics have lengths  $l_a, l_b, l_c$ .

Furthermore, the Y-pieces are the fundamental building blocks for higher order string vertices and reflected surfaces. So, it is reasonable to expect there are some close connections between them.

However, the connection is not straightforward. As discussed in last section, the boundary lengths of the string vertices are constrained to be the same while those of reflected surfaces are allowed to be different. A more serious problem is that the boundary lengths of the (quantum) string vertices have an upper bound  $L \leq L_*$ , but those of reflected surfaces have a lower bound  $S_R > 2L_*$ . We summarize these differences in Fig. (10) and the table,

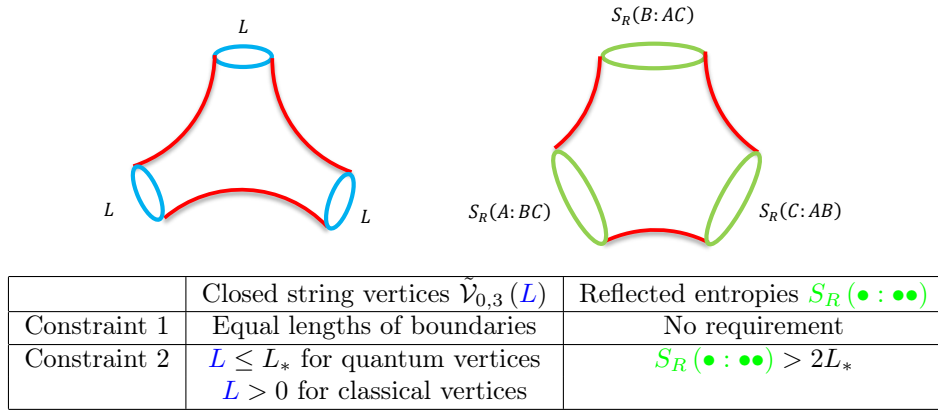


Figure 10: Differences of Y-pieces in two theories.

One might be puzzled why we introduce the string vertices to complicate the story. It looks that the Y-pieces and surfaces built on them are sufficient to construct the reflected surfaces, without the two strict constraints imposed by the string vertices. The reasons are three folds:

1. Though the classical string vertices allow any boundary geodesic length, they are only applicable to tree diagrams. To see this, let us recall the BV equation

$$\partial\mathcal{V} + \hbar\Delta\mathcal{V} + \frac{1}{2}\{\mathcal{V}, \mathcal{V}\} = 0.$$

In the classical limit  $\hbar \rightarrow 0$ , the second term  $\hbar\Delta\mathcal{V}$  disappears, and  $\mathcal{V} = \sum_{g,n} \hbar^g \mathcal{V}_{g,n} \rightarrow \mathcal{V} = \sum_{n \geq 3} \mathcal{V}_{0,n}$ . So, we will mainly discuss the quantum vertices and mention the classical limits when needed.

For the string vertices, BV equation = upper bounded hyperbolic surfaces:  $L \leq L_*$ . On the other hand, the reflected surfaces are lower bounded hyperbolic surfaces:  $S_R > 2L_*$ , constrained from the mutual information. Both objects are thus subsets of hyperbolic surfaces. Therefore, building connections between them is interesting and informative. One can anticipate some nontrivial results emerged from the connections.

2. The string vertices respect the dynamical equation, namely the BV equation (2.1). So, the string vertices provide us a practical approach to figure out dynamical properties of the reflected surfaces and entropies.
3. Through the connection, it is possible to build in CFT the holographic duals of the operations  $\Delta$  and  $\{, \}$ .

We first show how to construct reflected surfaces from string vertices, and then address the equal length restriction of the string vertices.

### 3.1 Construct reflected surfaces from string vertices

In this subsection, we present three examples to show how to construct the bulk geometries of multipartite canonical purification from the string vertices  $\mathcal{V}_{0,3}(L)$ . *Since a hyperbolic Riemann surface has different decomposition patterns, our constructions are far from unique.*

#### Example 1

Let us start with Fig. (11), the X-piece  $\tilde{\mathcal{V}}_{0,4}(L)$ , constructed by gluing two Y-pieces along the blue geodesic boundary  $\sigma$ .

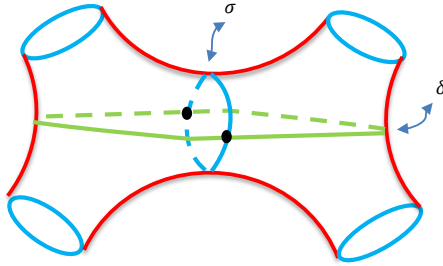


Figure 11: Gluing two string Y-pants to get X-piece.

According to Theorem 4, the X-piece is uniquely fixed by the blue geodesics, and we have:

**Corollary 5:** Considering two closed geodesics with lengths  $\sigma$  and  $\delta$  on a X-piece<sup>2</sup>, if  $\sigma$  and  $\delta$  intersect twice, we have  $\max\{\sigma, \delta\} > 2L_*$ . This bound is sharp [18].

This result naturally combines the bounds of two theories together:  $L \leq L_*$  in string vertices and  $S_R > 2L_*$  in entanglement, and it makes it possible to establish connections between two theories. More specifically, the quantitative relation between the values of  $\sigma$  and  $\delta$  is ([20], Theorem 2.3.4 (i)):

$$\cosh \frac{\sigma}{2} = \sinh \frac{\delta}{4} \sinh \frac{\sigma}{4}. \quad (3.19)$$

It is easy to derive that  $\delta$  has a minimum,

$$\delta = 4 \operatorname{arcsinh} \left( \frac{\cosh \sigma/2}{\sinh \sigma/4} \right) \geq 4 \operatorname{arcsinh}(2\sqrt{2}) \equiv \delta_{min} > S_{Rmin} \equiv 4 \operatorname{arcsinh}(1) = 2L_*. \quad (3.20)$$

---

<sup>2</sup>We use the same notations for the lengths of the curves

Note there is a *nontrivial* gap between the minimal values  $\delta_{min}$  and  $S_{Rmin}$ . Therefore, whatever the length of the blue boundary geodesics is, the green geodesic is always a valid reflected surface which indicates an up-down entanglement<sup>3</sup>. This realization provides a better option for the bulk interpretations for the reflection entropies.

In the classical theory, if the length of  $\sigma$  is also larger than  $2L_*$ , Fig. (11) basically represents a quadripartite reflected surface with four  $S_R(\bullet : \bullet \bullet \bullet) = \sigma$ , one  $S_R(\bullet \bullet : \bullet \bullet) = \sigma$  and one  $S_R(\bullet \bullet : \bullet \bullet) = \delta$ .

Note that in quantum theory, blue geodesics  $\sigma < L_*$ , so they do not contribute to the reflected entropy and the corresponding entanglement wedges disappear. We are therefore only left with the up-down bipartite entanglement  $S_R(\bullet : \bullet) = \delta$ , namely the green geodesic, as illustrated in Fig. (12), where the right panel collapses to the left panel. From eq. (3.19), a quantitative relation between the boundary length of the string vertices  $L = \sigma$  and the reflected entropy  $S_R(A : B) = \delta$  is

$$S_R(A : B) = 4 \operatorname{arcsinh} \frac{\cosh \frac{L}{2}}{\sinh \frac{L}{4}}, \quad (3.21)$$

$$L = 4 \operatorname{arcsinh} \left[ \frac{1}{4} \left( \sinh \frac{S_R}{4} \pm \sqrt{\sinh^2 \frac{S_R}{4} - 8} \right) \right]. \quad (3.22)$$

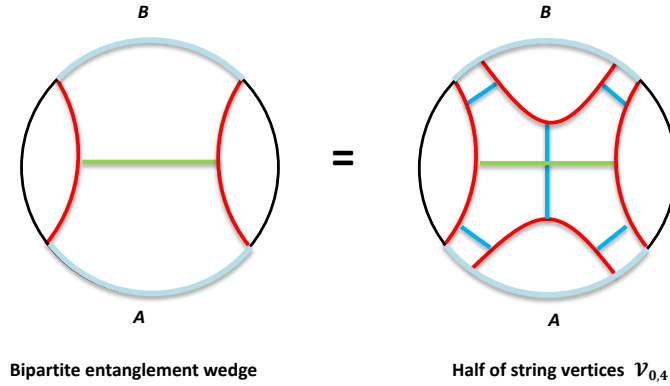


Figure 12: A quantum X-piece represents a bipartite reflected surface. Since the length of the blue geodesics is smaller than  $L_*/2$ , they can not be reflected surfaces and no entanglement wedge exists. The only legitimate reflected surface is the green geodesic which indicates an up-down entangling.

#### The gap between $\delta_{min}$ and $S_{Rmin}$ , generalized reflected entropy

In eq. (3.20), there exists a nontrivial gap between the minimal values of  $\delta_{min} = 4 \operatorname{arcsinh}(2\sqrt{2})$  and  $S_{Rmin} = 2L_* = 4 \operatorname{arcsinh}(1)$ . It is very instructive to study the origin of this gap.

The reason is that the hyperbolic string vertices with explicit local coordinates provide non-perturbative corrections to the reflected entropies. In [10], it shows that the hyperbolic three-string vertex reduces to the naive three-string vertex as the geodesic boundaries  $L$ 's approach zero. It is not difficult to generalize this result

<sup>3</sup>Of course, one can rotate the X-piece by 90 degree and switch the roles of  $\sigma$  and  $\delta$ . In this case, we always have a left-right entanglement.

to the four-string vertex. Under this limit, the outer four geodesic boundaries  $L$ 's of  $\mathcal{V}_{0,4}$  go to zero, one then gets  $\delta_{min} \rightarrow S_{Rmin} = 2L_*$  (Proposition 3.1. in ref. [22]), as depicted in Fig. (13). It therefore indicates that the real bulk dual of the reflected entropy is not the reflected surface (hyperbolic string vertex), but the Moosavian-Pius surface! Since the Moosavian-Pius surface is a limit of the hyperbolic string vertex, the hyperbolic string vertex should be dual to a *generalized* reflected entropy in the CFT, which has the reflected entropy as a limit.

This limiting behavior is also consistent with a bulk interpretation of the mutual information:

$$\begin{aligned} I(A : B) &= S_A + S_B - S_{AB} \\ &= \text{Area}(\gamma_A) + \text{Area}(\gamma_B) - \text{Area}(2\gamma_{AB}). \end{aligned} \quad (3.23)$$

Therefore, the hyperbolic string vertices provide alternative quantum corrections to the entanglement entropy. Since the adjacent red geodesics cannot join together at one point on the boundary in Fig. (12), the quantum gravitational effects (originated from closed strings) in the bulk will introduce a minimal observable length near the boundary, and then modify the minimal value of the reflected entropy  $S_{Rmin}$  to  $\delta_{min}$  in eq. (3.20).

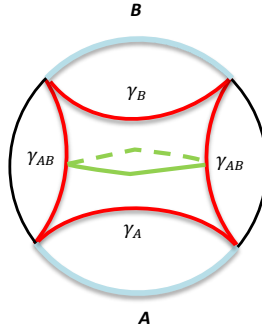


Figure 13: Naive four-string vertex: it is a limit of Costello-Zwiebach hyperbolic string vertex.

This gap is also found in the reflected entropy of the three-boundary wormholes [25]. Referring to Fig. (14), the left panel describes a three-boundary wormhole. The black circles denote the three asymptotic boundaries. The blue circles  $L_A, L_B, L_C$  are geodesics of length  $\sigma$ . The reflected entropy  $S_R(A : B)$  for the bipartite mixed state  $(A, B, C)$  can be calculated by canonical purification. The process of canonical purification is similar to that of CFT: 1) Prepare a copy of the Y-piece, say  $(A^*, B^*, C)$ ; 2) Glue these two Y-pieces along the blue geodesic  $L_C$ , which denotes to trace out  $C$ ; 3) The reflected surface is the minimal geodesic between  $AA^*$  and  $BB^*$ ,  $S_R(A : B) = S(AA^*)_{\sqrt{\rho_{AB}}}$ .

Looking at the right panel of Fig. (14), there are three reflected surface candidates separating  $AA^*$  from  $BB^*$ . Since  $(L_A + L'_A) = (L_B + L'_B) = 2\sigma \leq 2L_*$  belongs to the disconnected phase, the only choice is  $S_R(A : B) = \delta$ . Therefore, the minimal value of the reflected entropy between  $A$  and  $B$  of the three-boundary wormhole is  $\delta_{min} = 4\text{arcsinh}(2\sqrt{2}) > 2L_*$ . One can refer to [26, 27] for further details of the wormhole reflected entropies.

So, the existence of the gap is not occasional. In order to understand the cause of this gap, careful studies on the (generalized) reflected entropy from CFT perspective is necessary in future works.

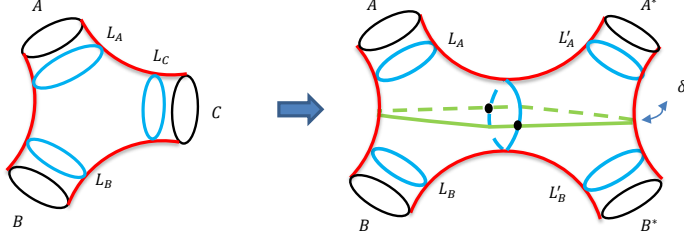


Figure 14: The canonical purification of three boundary wormhole.

### Example 2

The second example, referring to Fig. (15), is to show how to build the bulk geometry of a tripartite system by string vertices. The classical construction is trivial: it is simply a Y-piece. Quantum construction needs a little work and has the following steps:

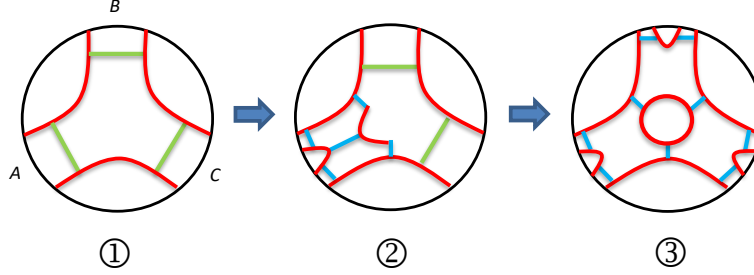


Figure 15: Rebuild tripartite canonical purification by string vertices  $\tilde{\mathcal{V}}_{1,6}$ . Note all green or blue geodesics have the same lengths.

1. Since the boundaries (blue) of the string vertices have equal length, the corresponding bipartite reflected entropies (green) have the same value  $S_R(A : BC) = S_R(B : AC) = S_R(B : AC) = s$ .
2. From example 1, the bulk geometry of a bipartite entanglement wedge can be replaced by a string vertex  $\tilde{\mathcal{V}}_{0,4}(L)$ , as illustrated by the middle panel.
3. Do the replacement for all three bipartite systems, we get a string vertex  $\tilde{\mathcal{V}}_{1,6}(L)$  by gluing three X-pieces, or equivalently speaking, six Y-pieces  $\tilde{\mathcal{V}}_{0,3}(L)$ .

Moreover, the string vertices  $\mathcal{V}_{1,6}(L)$  and reflected entropy are mutually computable:

$$\begin{aligned}
 S_R(\bullet : \bullet\bullet) &= s = 4 \operatorname{arcsinh} \frac{\cosh \frac{L}{2}}{\sinh \frac{L}{4}}, \\
 \mathcal{V}_{1,6}(L) &= \mathcal{V}_{1,6} \left( 4 \operatorname{arcsinh} \left[ \frac{1}{4} \left( \sinh \frac{s}{4} - \sqrt{\sinh^2 \frac{s}{4} - 8} \right) \right] \right).
 \end{aligned} \tag{3.24}$$



### Example 3

The third example is a bipartite system for a thermal state of  $\text{CFT}_2$ . Unlike the previous two examples, the bulk dual of this state intrinsically has a black hole located at the center of the Poincare disk. The black hole introduces a genus after purification, see Fig. (16), which invalidates classical constructions. So, this reflected surface can only be constructed quantum mechanically.

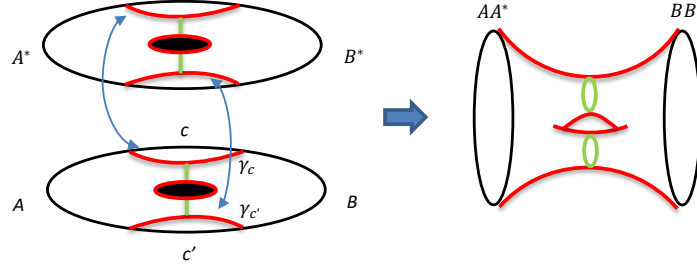


Figure 16: Canonical purification for a thermal state.

To construct the bulk geometry with string vertices, we have the following steps as illustrated in Fig. (17):

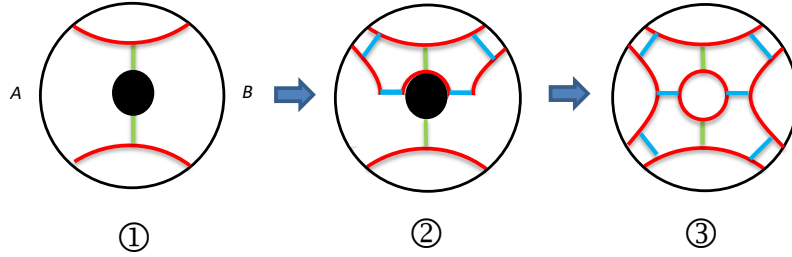


Figure 17: Bipartite canonical purification with a black hole can be built by  $\mathcal{V}_{1,4}$ .

1. Two disconnected green geodesics in the left panel has the total length  $S_R(A : B) = 2s$ .
2. From example 1, we can replace each green geodesic by a string vertices  $\tilde{\mathcal{V}}_{0,4}(L)$ .
3. Gluing two  $\tilde{\mathcal{V}}_{0,4}(L)$  along blue boundaries, we see that the bulk geometry can be built by a string vertex  $\mathcal{V}_{1,4}(L)$ .

From eq. (3.19), we have

$$\begin{aligned}
 S_R(A : B) &= 2s = 8 \text{arc sinh} \frac{\cosh \frac{L}{2}}{\sinh \frac{L}{4}}, \\
 \mathcal{V}_{1,4}(L) &= \mathcal{V}_{1,4} \left( 4 \text{arc sinh} \left[ \frac{1}{4} \left( \sinh \frac{s}{4} - \sqrt{\sinh^2 \frac{s}{4} - 8} \right) \right] \right).
 \end{aligned} \tag{3.25}$$

Moreover, by using eq. (2.3), the area  $A$  of the black hole's horizon also can be fixed by the string vertices:

$$A = 2\text{arc cosh} \frac{\cosh \frac{L}{2}}{\cosh \frac{L}{2} - 1}. \quad (3.26)$$

### 3.2 Remove the equal length restriction

Since the boundary geodesics of string vertex  $\tilde{\mathcal{V}}_{0,3}(L)$  has equal length  $L < L_*$ , one may worry the reflected surfaces built on it are too restricted. To clarify this problem, we consider the canonical purification of a pentapartite mixed state. The dual bulk geometry can be rebuilt by five X-pieces, as sketched in Fig. (18). Since the geodesic lengths of string vertices have the same value  $L$ , all bipartite reflected entropies  $S_R(\bullet : \bullet \bullet \bullet \bullet)$  (solid green lines) near the boundary are identical. Remarkably, there emerges a new class of bipartite reflected entropies (green dashed line) which have different values  $S_R(\bullet \bullet : \bullet \bullet \bullet) \neq S_R(\bullet : \bullet \bullet \bullet \bullet)$ .

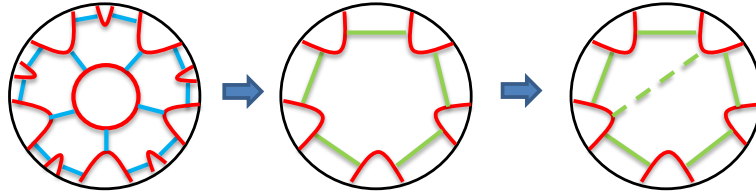


Figure 18: The blue geodesics disappear when we calculate the entanglement wedge cross sections since  $L < L_*$ . In addition to the near boundary bipartite reflected surfaces  $S_R(\bullet : \bullet \bullet \bullet \bullet)$  (solid green lines), a new class of bipartite reflected entropies (green dashed line) emerges  $S_R(\bullet \bullet : \bullet \bullet \bullet) \neq S_R(\bullet : \bullet \bullet \bullet \bullet)$ .

It is easy to understand that by adding more X-pieces, various reflected surfaces can be constructed. Particularly, one general situation is exhibited by Fig. (19), where all pieces are right-angled equilateral hexagons. The sides of these hexagons are all equal [28]. Obviously, each hexagon relates different disk boundary regions when we prolong the sides to the boundary of the Poincare disk. By selecting appropriate hexagons, one can get, say, arbitrary bipartite surfaces.

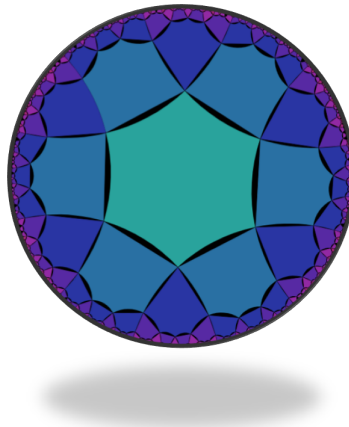


Figure 19: The sides of all hexagons are equal. By prolonging the sides to the boundary, each hexagon corresponds to a different region on the boundary. One thus can get different reflected entropies by selecting different hexagons.

Before closing this section, let us give some remarks:

#### Holographic realization of phase transition

We have mentioned that there is a discontinuity of  $S_R(A : B)$  at  $2L_*$ , where  $S_R(A : B)$  jumps from  $2L_*$  to 0 abruptly, as shown by Fig. (9). Referring to the X-piece (11) and eq. (3.20), we can see that this process basically corresponds to an exchange of the roles of  $\sigma$  and  $\delta$ . For a surface, there are different pants decompositions. For example, one can decompose an X-piece in an up-down or left-right way, as in Fig. (20). These two different decompositions indicate different entangling directions. Mathematically, this is called an A-move [44]. In other words, the phase transition between the disconnected phase and the connected phase is actually an A-move.

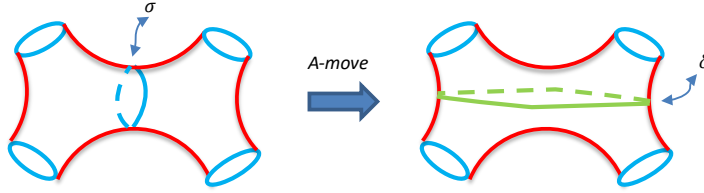


Figure 20: A-move of the X-piece.

## 4 Preliminary evidence

In order to reinforce the connections between two theories, in this section, we present an evidence of it. As mentioned by Costello and Zwiebach [8], the hyperbolic metrics can also be used in the open string field theory. In the classical limit, the three-open-string vertex can be constructed with a hyperbolic hexagon  $L/2, \vartheta, L/2, \vartheta, L/2, \vartheta$  directly (See Fig. (1)), followed by grafting three semi-infinite strips of width  $L/2$  as the external legs on the boundaries. It is then obvious that, the three-closed-string vertices are obtained by gluing two three-open-string vertices. This is precisely the pattern of canonical purification. Therefore, to close the logic chain between entanglement theory and string field theory, there should be an inference that, some (if not all) properties of the closed string field theory (CSFT) can be constructed by purification from the open string field theory (OSFT) with mixed state:

$$\begin{array}{ccccc}
 & \text{Entanglement} & & & \\
 \text{EE :} & \text{wedge cross section} & \xrightarrow{\text{Purified}} & & \text{Reflected surface} \\
 & \text{(mixed state)} & & & \\
 & \downarrow & & & \\
 \text{String :} & \text{Open string field theory} & \xrightarrow{\text{Purified}} & & \text{Closed string field theory} \\
 & \text{(mixed state)} & & & 
 \end{array}$$

To build the connections between classical OSFT and purification of entanglement, there are two points need to be considered: 1) Classically, hyperbolic OSFT is a non-polynomial theory, therefore its vertices do not satisfy the strict associativity [32]. This implies that there exist  $n \geq 4$  open-string vertices which can be obtained by cutting the closed string vertices  $\mathcal{V}_{0,n}$  along  $\vartheta$ 's. 2) In the quantum version, the loop diagrams of open strings

naturally include closed strings. It is inconsistent to consider OSFT only. We leave this construction to the future work.

The following result has been obtained in [33]. We simply present the main conclusions here.

In order to study how to achieve the purification in string field theory, we first introduce the Thermofield Double (TFD) state. In QFT, the Hamiltonian  $H$  and its eigenstate  $|n\rangle$  are given by

$$H |n\rangle = E_n |n\rangle. \quad (4.27)$$

The TFD formalism is to double the degrees of freedom of the thermal or mixed state  $\rho = e^{-\beta H}$ , and then obtain a larger pure state. The TFD state of this doubled system is defined as

$$|TFD\rangle = \frac{1}{\sqrt{Z(\beta)}} \sum_n e^{-\beta E_n/2} |n\rangle_1 |n\rangle_2, \quad (4.28)$$

which is a pure state in the new system. The corresponding reduced density matrix is given by  $\rho_{total} = |TFD\rangle \langle TFD|$ . It is easy to check that when the system 2 is traced out, the reduced density matrix becomes  $\rho_1 = \text{Tr}_2 \rho_{total} = e^{-\beta H_1}$  which agrees with the original thermal state. This procedure is called the purification of the thermal state. A comprehensive introduction can be found in [34] and references therein. In the following discussions, we will denote  $|n\rangle_1 \equiv |n\rangle$  and its copy  $|n\rangle_2 \equiv |\tilde{n}\rangle$ . Using the new notations, the Hamiltonian  $\hat{H}$  of the doubled system can be defined as:

$$\hat{H} \equiv H - \tilde{H}. \quad (4.29)$$

In addition, the TFD formalism allows us to obtain the operators  $\tilde{X}, \tilde{Y}, \dots$  from  $X, Y, \dots$  by the tilde conjugation rules [35]:

$$\begin{aligned} (XY)^\sim &= \tilde{X}\tilde{Y}, \\ (cX + Y)^\sim &= c^* \tilde{X} + \tilde{Y}, \\ (X^\dagger)^\sim &= \tilde{X}^\dagger, \\ [\tilde{X}, Y] &= 0, \\ (\tilde{X})^\sim &= \epsilon X, \end{aligned} \quad (4.30)$$

where  $c^*$  relates to the  $c^*$ -algebra and  $\epsilon = +1 (-1)$  for commuting (anti-commuting) fields.

Now, consider the Witten's cubic OSFT action [36],

$$S[\Phi] = \frac{1}{2} \langle \Phi, Q_B \Phi \rangle + \frac{g}{3} \langle \Phi, \Phi, \Phi \rangle, \quad (4.31)$$

where  $Q_B$  is the BRST operator,  $g$  is the open string coupling constant, and  $\langle \cdot, \cdot \rangle$  and  $\langle \cdot, \cdot, \cdot \rangle$  are 2-point and 3-point vertices. The state of open string field can be expanded in the Fock space basis:

$$|\Phi\rangle = \int \frac{d^D k}{(2\pi)^D} (T(k) + A_\mu(k) \alpha_{-1}^\mu + \dots) |\Omega\rangle, \quad (4.32)$$

where  $T$  denotes the tachyon field,  $A_\mu$  denotes the photon field,  $|\Omega\rangle = c_1 |0; k\rangle$  is the vacuum of the Fock space, and  $\alpha_{-1}^\mu$  is the Fourier mode of a string  $X^\mu(\tau, \sigma)$ . To calculate the bracket in (4.31), it is useful to define the reflector state. Using  $|\Phi_i\rangle \in \mathcal{H}_{CFT}$  to denote a basis for states and its dual  $\langle\Phi^i| \in \mathcal{H}_{CFT}^*$  such that  $\langle\Phi^i|\Phi_j\rangle = \delta_j^i$ , the correlation is given by

$$\langle\Phi_i, \Phi_j\rangle \equiv \langle R_{12}|\Phi_i\rangle_{(1)} |\Phi_j\rangle_{(2)}, \quad (4.33)$$

where  $\langle R_{12}| \in \mathcal{H}_{CFT}^* \otimes \mathcal{H}_{CFT}^*$ .

We now show how OSFT relates to CSFT after using the TFD formalism. In this formalism, the original one-open string vacuum state is doubled:

$$|\Omega\rangle = c_1 |0; k\rangle, \quad |\tilde{\Omega}\rangle = \tilde{c}_1 |\tilde{0}; \tilde{k}\rangle. \quad (4.34)$$

Using these states, the total vacuum state of the doubled system is defined as

$$|\Omega\rangle\rangle \equiv |\Omega\rangle \otimes |\tilde{\Omega}\rangle = c_1 |0; k\rangle \otimes \tilde{c}_1 |\tilde{0}; -k\rangle, \quad (4.35)$$

where  $\tilde{k} = -k$  comes from the requirement that the purified state  $|\Omega\rangle\rangle$  must equal its tilde conjugate:  $|\widetilde{|\Omega\rangle\rangle} = |\Omega\rangle\rangle$ . We also have

$$(L_0 - 1)|\Omega\rangle\rangle = 0, \quad (\tilde{L}_0 - 1)|\Omega\rangle\rangle, \quad (L_0 - \tilde{L}_0)|\Omega\rangle\rangle = 0. \quad (4.36)$$

Based on the definition of the vacuum state, the states of open string field are doubled:

$$\begin{aligned} |\Phi\rangle\rangle &= \int \frac{d^D k}{(2\pi)^D} (T(k) + A_\mu(k) \alpha_{-1}^\mu + B_\mu(k) \tilde{\alpha}_{-1}^\mu \cdots) |\Omega\rangle\rangle, \\ |\tilde{\Phi}\rangle\rangle &= \int \frac{d^D k}{(2\pi)^D} (\tilde{T}(k) + \tilde{A}_\mu(k) \tilde{\alpha}_{-1}^\mu + \tilde{B}_\mu(k) \alpha_{-1}^\mu \cdots) |\Omega\rangle\rangle. \end{aligned} \quad (4.37)$$

Therefore, the kinetic term of OSFT can be extended with the TFD formalism to:

$$\hat{S}[\Phi, \tilde{\Phi}] = S[\Phi] - \tilde{S}[\tilde{\Phi}]. \quad (4.38)$$

The corresponding reflector is  $\langle\langle R_{12}| \equiv \langle R_{12}| \otimes \langle R_{12}|$  which also equals its tilde conjugate. More explicitly, the free-OSFT action is

$$\hat{S}[\Phi, \tilde{\Phi}] = \frac{1}{2} \langle\langle \Phi, Q_B \Phi \rangle\rangle - \frac{1}{2} \langle\langle \tilde{\Phi}, \tilde{Q}_B \tilde{\Phi} \rangle\rangle, \quad (4.39)$$

with equations of motion:

$$Q_B |\Phi\rangle\rangle = 0, \quad \tilde{Q}_B |\tilde{\Phi}\rangle\rangle = 0, \quad (4.40)$$

which are the same as the physical condition in the BRST quantization. To relate this action (4.39) with the action of CSFT, one introduces the generally entangled ground states, namely  $\Omega$ -states, which is defined by

$$\left(L_0 - \tilde{L}_0\right) |\Omega(\theta)\rangle\rangle = 0, \quad |\Omega(\theta)\rangle\rangle = |\widetilde{\Omega(\theta)}\rangle\rangle, \quad (4.41)$$

where  $\theta$  denotes the level of a component field which characterizes the vacuum. Using  $\Omega$ -states, the equations of motion of (4.39) give

$$Q_B \pm \tilde{Q}_B |\Omega(\theta)\rangle\rangle = 0. \quad (4.42)$$

The “+” sign gives the equations of motion of free-CSFT and the first equation of (4.41) is precisely the level-matching condition. Moreover,  $|\Omega(\theta)\rangle\rangle$  also can be expanded in  $|\Omega\rangle\rangle$ :

$$|\Omega(\theta)\rangle\rangle = \int \frac{d^D k}{(2\pi)^D} (T(k) + C_{\mu\nu}(k) \alpha_{-1}^\mu \tilde{\alpha}_{-1}^\nu \cdots) |\Omega\rangle\rangle, \quad (4.43)$$

where  $t(k) = \tilde{t}(k)$ ,  $C_{\mu\nu}(k) = \tilde{C}_{\nu\mu}(k)$ , and  $\theta$  denotes the level of the component field  $(t, C_{\mu\nu}, \dots)$ .  $C_{\mu\nu}$  can be decomposed into  $g_{\mu\nu} + b_{\mu\nu} + \phi\eta_{\mu\nu}$  to include the closed string massless sector. In addition, from the equations of motion (4.42), it is easy to figure out the action:

$$\hat{S}_{\text{Canonical}}[\Omega] = \frac{1}{2} (\langle\langle R_{12}|\Omega\rangle\rangle) \hat{c}_0 (Q_B + \tilde{Q}_B) |\Omega\rangle\rangle, \quad (4.44)$$

which is the free-CSFT action. Therefore,  $\Omega$ -states can be seen as the asymptotic states of free-CSFT. For the higher order interacting vertices, the derivations are not easy. As an alternative, one can check the S-matrix and expect the results to agree with the closed string. The detailed discussions can be found in [33].

## 5 Hyperbolic closed string vertices as spacetime building blocks?

In the previous discussions, we have proposed a connection between the reflected entropy/surfaces and hyperbolic string vertices. Since it is widely believed that the spacetime structure could be generated by the entanglement entropy through the dual surfaces, it is natural to ask if the spacetime structure could directly emerge from the hyperbolic string vertices. The advantage of the hyperbolic string vertices approach is that we have a dynamical equation, the BV master equation, to control the generating process.

To explain this idea more explicitly, let us consider the disentangling process of a bipartite system in Fig. (21). In this mixed state, once regions  $A$  and  $B$  are fixed, the reflected surface  $S_R(A : B) > 2L_*$  is also fixed. How to disentangle regions  $A$  and  $B$  without changing the boundary geometry? This is different from the phase transition discussed in section 2.2 where regions  $A$  and  $B$  are changed. Following the arguments about emergent spacetime introduced in [37], the only way to realize the disentanglement is to disconnect the spacetime into two separate parts.

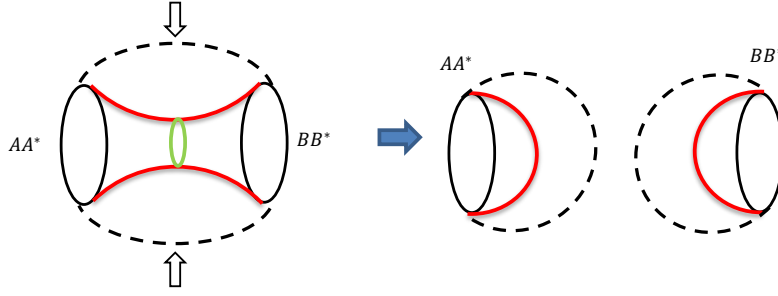


Figure 21: Disconnect a bipartite mixed state into two separate parts in the picture of entanglement entropy.

On the other hand, we can consider this process from the perspective of hyperbolic closed string vertices, let us focus on the simplest case: 2D universes. It is verified and well understood that the 2D universes can be described by string theory. The sum-over-two-geometries of string field theory can be considered as a theory of splitting and joining of 2D baby universes [38, 39]. Therefore, the hyperbolic string vertices of CSFT indeed play the role of spacetime building blocks of interacting 2D universes. In Fig. (22) we present how a joining of universes can be viewed as the BV gluing process of hyperbolic string vertices  $\mathcal{V}_{0,3}$ : we remove two disks of each three-sphere by cutting along the blue geodesics and then glue them together. This operation is also discussed in holographic baby universes in ref. [40]. The process is controlled by the BV equation, and the only way to destroy the entanglement is to disconnect the spacetime into two separate parts, which is triggered by tachyon condensation [41].

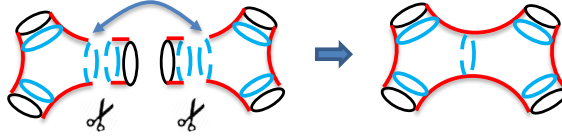


Figure 22: Creation of a baby universe by gluing two hyperbolic string vertices  $\mathcal{V}_{0,3}$ .

Based on this observation, we can complete a triangular relation as depicted in Fig. (23). First, it is known that the string vertices correspond to the splitting and joining of 2D baby universes, which is proposed by Giddings and Strominger (1 in Fig. (23)) [39]. Then, Raamsdonk argues that the splitting and joining of spacetime relate to the quantum entanglement (2 in Fig. (23)) [37]. Finally, our discussions of the connections between reflected entropies and hyperbolic string vertices complete this triangle (3 in Fig. (23)).

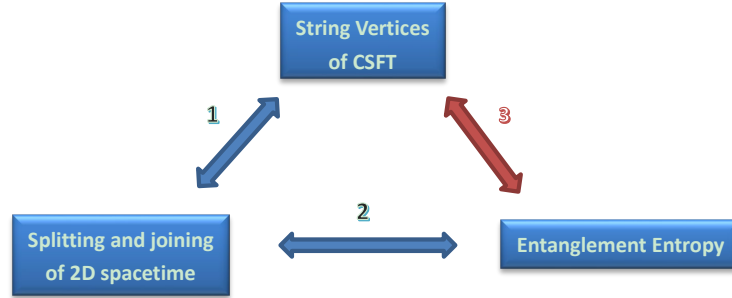


Figure 23: Triangular relation: 1. Giddings and Strominger’s baby universes. 2. Van Raamsdonk’s conjecture. 3. Connections between reflected entropies and hyperbolic string vertices.

Then, it is reasonable to conjecture that higher dimensional  $D > 2$  spacetime also can be affected by the interactions of closed strings. Of course, there are many works need be done to verify this point. As a result, *spacetime tells worldsheet how to move, and worldsheet tells spacetime how to glue.*

## 6 Conclusion and discussions

In short, we proposed close connections between the reflected entropies/surfaces of the multipartite mixed states of  $\text{CFT}_2$  and the hyperbolic string vertices of CSFT. We found that the reflected entropies could be determined by hyperbolic string vertices and vice versa. We consequently conjectured that the hyperbolic string vertices can play a major role in building spacetime.

Some remarks and future works are as follows.

- Cho has generalized constructions of the closed string vertices to the open-closed string vertices [9]. It is worth extending our results to find the boundary dual of the open-closed string vertices. Are they some new entanglement quantities or existing ones?
- In subsection 3.1, we explained what accounts for the gap between  $\delta_{min}$  and  $S_{Rmin}$ . Note that  $\delta_{min}$  is for the *geodesic* bounded hyperbolic surfaces, which are precisely the reflected surfaces or the hyperbolic string vertices. Nevertheless,  $S_{Rmin}$  is for the *horocycle* bounded hyperbolic surfaces which are the Moosavian-Pius surfaces. Therefore, from this point of view, the bulk dual of the reflected entropy of CFT is not the reflected surface, but the Moosavian-Pius surface!

Given that Moosavian-Pius surface is a limit of the reflected surface or hyperbolic string vertex, we are led to believe that there should exist a *generalized* reflected entropy in the CFT which is the real dual of the reflected surface. This *generalized* reflected entropy has the reflected entropy as its limit.

- The random stabilizer tensor networks (RSTN) are studied in ref. [42]. Canonical purification for the tensor networks are considered in ref. [43]. As we showed in section 5, the tensor networks share great similarity with the interactions of hyperbolic string vertices, it is of interest to study their relation more carefully and deeply.



- Geometric master equation controls various interactions (such as taking boundary, or sewing together) between vertices  $\mathcal{V}_{g,n}$ . Since  $\mathcal{V}_{g,n}$  is connected to the canonical purification of mixed states. There could be a boundary version of geometric master equation which tells us how two systems to entangle with each other.
- Based on our results, it is possible to define the moduli space of entanglement entropy. Since hyperbolic string vertices satisfy the BV equation on the moduli space, it is possible to get modularized equations of motion of the CFT.
- The connections between the canonical purification of the multipartite mixed states of  $\text{CFT}_2$  and the hyperbolic string vertices of CSFT are special cases of  $\text{AdS}_3/\text{CFT}_2$ , since the closed string vertices possess the hyperbolic geometry intrinsically. In addition, it indicates that  $\text{AdS}/\text{CFT}$  has been encoded in string theory, since the string amplitudes can be calculated by CFT on punctured Riemann surfaces or hyperbolic string vertices in their bulk.
- In this paper, we are only concerned with  $d = 2$  case. one might wonder if it is possible to build higher dimensional bulk geometries with string vertices. We anticipate that higher-dimensional fundamental objects: branes, might achieve this purpose.

**Acknowledgements** We are deeply indebted to Amr Ahmadain, Aron Wall and Zihan Yan for illuminating discussions. This work is supported in part by the NSFC (Grant No. 12105191, 11947225 and 11875196). HW is supported by the International Visiting Program for Excellent Young Scholars of SCU.

## References

- [1] H. Hata and B. Zwiebach, “Developing the covariant Batalin-Vilkovisky approach to string theory,” *Annals Phys.* **229**, 177 (1994) doi:10.1006/aphy.1994.1006 [hep-th/9301097].
- [2] A. Sen and B. Zwiebach, “Quantum background independence of closed string field theory,” *Nucl. Phys. B* **423**, 580 (1994) doi:10.1016/0550-3213(94)90145-7 [hep-th/9311009].
- [3] A. Sen and B. Zwiebach, “Background independent algebraic structures in closed string field theory,” *Commun. Math. Phys.* **177**, 305 (1996) doi:10.1007/BF02101895 [hep-th/9408053].
- [4] B. Zwiebach, “Closed string field theory: Quantum action and the B-V master equation,” *Nucl. Phys. B* **390**, 33 (1993) doi:10.1016/0550-3213(93)90388-6 [hep-th/9206084].
- [5] B. Zwiebach, “How covariant closed string theory solves a minimal area problem,” *Commun. Math. Phys.* **136**, 83-118 (1991) doi:10.1007/BF02096792
- [6] S. F. Moosavian and R. Pius, “Hyperbolic geometry and closed bosonic string field theory. Part I. The string vertices via hyperbolic Riemann surfaces,” *JHEP* **08**, 157 (2019) doi:10.1007/JHEP08(2019)157 [arXiv:1706.07366 [hep-th]].

- [7] S. F. Moosavian and R. Pius, “Hyperbolic geometry and closed bosonic string field theory. Part II. The rules for evaluating the quantum BV master action,” JHEP **08**, 177 (2019) doi:10.1007/JHEP08(2019)177 [arXiv:1708.04977 [hep-th]].
- [8] K. Costello and B. Zwiebach, “Hyperbolic string vertices,” JHEP **02**, 002 (2022) doi:10.1007/JHEP02(2022)002 [arXiv:1909.00033 [hep-th]].
- [9] M. Cho, “Open-closed Hyperbolic String Vertices,” JHEP **05**, 046 (2020) doi:10.1007/JHEP05(2020)046 [arXiv:1912.00030 [hep-th]].
- [10] A. H. Firat, “Hyperbolic three-string vertex,” doi:10.1007/JHEP08(2021)035 [arXiv:2102.03936 [hep-th]].
- [11] H. Sonoda and B. Zwiebach, “COVARIANT CLOSED STRING THEORY CANNOT BE CUBIC,” Nucl. Phys. B **336**, 185-221 (1990) doi:10.1016/0550-3213(90)90108-P
- [12] S. Ryu and T. Takayanagi, “Holographic derivation of entanglement entropy from AdS/CFT,” Phys. Rev. Lett. **96**, 181602 (2006) doi:10.1103/PhysRevLett.96.181602 [hep-th/0603001].
- [13] T. Takayanagi and K. Umemoto, “Entanglement of purification through holographic duality,” Nature Phys. **14**, no. 6, 573 (2018) doi:10.1038/s41567-018-0075-2 [arXiv:1708.09393 [hep-th]].
- [14] S. Dutta and T. Faulkner, “A canonical purification for the entanglement wedge cross-section,” JHEP **03**, 178 (2021) doi:10.1007/JHEP03(2021)178 [arXiv:1905.00577 [hep-th]].
- [15] N. Engelhardt and A. C. Wall, “Coarse Graining Holographic Black Holes,” JHEP **1905**, 160 (2019) doi:10.1007/JHEP05(2019)160 [arXiv:1806.01281 [hep-th]].
- [16] N. Bao and N. Cheng, “Multipartite Reflected Entropy,” JHEP **1910**, 102 (2019) doi:10.1007/JHEP10(2019)102 [arXiv:1909.03154 [hep-th]].
- [17] J. Chu, R. Qi and Y. Zhou, “Generalizations of Reflected Entropy and the Holographic Dual,” JHEP **03**, 151 (2020) doi:10.1007/JHEP03(2020)151 [arXiv:1909.10456 [hep-th]].
- [18] T. Gauglhofer, K.-D. Semmler, “Trace coordinates of Teichmüller space of Riemann surfaces of signature (0,4),” Conform. Geom. Dyn. **9** (2005), 46-75.
- [19] N. Bao, A. Chatwin-Davies and G. N. Remmen, “Entanglement of Purification and Multiboundary Wormhole Geometries,” JHEP **1902**, 110 (2019) doi:10.1007/JHEP02(2019)110 [arXiv:1811.01983 [hep-th]].
- [20] P. Buser, “Geometry and spectra of compact Riemann surfaces,” Birkhauser Boston 1992.
- [21] N. Bao, A. Chatwin-Davies and G. N. Remmen, “Entanglement Wedge Cross Section Inequalities from Replicated Geometries,” JHEP **07**, 113 (2021) doi:10.1007/JHEP07(2021)113 [arXiv:2106.02640 [hep-th]].
- [22] T. Gauglhofer and H. Parlier, “Minimal length of two intersecting simple closed geodesics,” manuscripta math. **122**, 321-339 (2007) doi:10.1007/s00229-006-0071-1 [math/0608049 [math.DG]].

- [23] B.M. Terhal, M. Horodecki, D.W. Leung and D.P. DiVincenzo, “The entanglement of purification,” J. Math. Phys. **43** (2002) 4286 [quant-ph/0202044].
- [24] M. Headrick, “Entanglement Renyi entropies in holographic theories,” Phys. Rev. D **82**, 126010 (2010) doi:10.1103/PhysRevD.82.126010 [arXiv:1006.0047 [hep-th]].
- [25] P. Hayden, O. Parrikar and J. Sorce, “The Markov gap for geometric reflected entropy,” JHEP **10**, 047 (2021) doi:10.1007/JHEP10(2021)047 [arXiv:2107.00009 [hep-th]].
- [26] C. Akers, N. Engelhardt and D. Harlow, “Simple holographic models of black hole evaporation,” JHEP **08**, 032 (2020) doi:10.1007/JHEP08(2020)032 [arXiv:1910.00972 [hep-th]].
- [27] T. Li, J. Chu and Y. Zhou, “Reflected Entropy for an Evaporating Black Hole,” JHEP **11**, 155 (2020) doi:10.1007/JHEP11(2020)155 [arXiv:2006.10846 [hep-th]].
- [28] The programme to plot the hyperbolic tiling can be found in the website: <http://www.malinc.se/noneuclidean/en/poincaretiling.php>
- [29] D. Brill, “Black holes and wormholes in (2+1)-dimensions,” Lect. Notes Phys. **537**, 143 (2000) [gr-qc/9904083].
- [30] B. Zwiebach, “Closed string field theory: An Introduction,” hep-th/9305026.
- [31] D. Stanford and L. Susskind, “Complexity and Shock Wave Geometries,” Phys. Rev. D **90**, no.12, 126007 (2014) doi:10.1103/PhysRevD.90.126007 [arXiv:1406.2678 [hep-th]].
- [32] M. R. Gaberdiel and B. Zwiebach, “Tensor constructions of open string theories. 1: Foundations,” Nucl. Phys. B **505**, 569-624 (1997) doi:10.1016/S0550-3213(97)00580-4 [arXiv:hep-th/9705038 [hep-th]].
- [33] M. Botta Cantcheff and R. J. Scherer Santos, “Thermofield dynamics extension of the open string field theory,” Phys. Rev. D **93**, no.6, 065015 (2016) doi:10.1103/PhysRevD.93.065015 [arXiv:1508.03603 [hep-th]].
- [34] T. Hartman, “Lectures on Quantum Gravity and Black Holes.” <http://www.hartmanhep.net/topics2015/>
- [35] A. E. Santana, A. Matos Neto, J. D. M. Vianna, F. C. Khanna, “Symmetry groups, density-matrix equations and covariant Wigner functions,” Physica A280 (2000) 405.
- [36] E. Witten, Nucl. Phys. B **268**, 253-294 (1986) doi:10.1016/0550-3213(86)90155-0
- [37] M. Van Raamsdonk, “Building up spacetime with quantum entanglement,” Gen. Rel. Grav. **42**, 2323-2329 (2010) doi:10.1142/S0218271810018529 [arXiv:1005.3035 [hep-th]].
- [38] A. G. Cohen, G. W. Moore, P. C. Nelson and J. Polchinski, “An Off-Shell Propagator for String Theory,” Nucl. Phys. B **267**, 143-157 (1986) doi:10.1016/0550-3213(86)90148-3
- [39] S. B. Giddings and A. Strominger, “Baby Universes, Third Quantization and the Cosmological Constant,” Nucl. Phys. B **321**, 481-508 (1989) doi:10.1016/0550-3213(89)90353-2

- [40] E. Gesteau and M. J. Kang, “Holographic baby universes: an observable story,” [arXiv:2006.14620 [hep-th]].
- [41] A. Adams, X. Liu, J. McGreevy, A. Saltman and E. Silverstein, “Things fall apart: Topology change from winding tachyons,” JHEP **10**, 033 (2005) doi:10.1088/1126-6708/2005/10/033 [arXiv:hep-th/0502021 [hep-th]].
- [42] P. Hayden, S. Nezami, X. L. Qi, N. Thomas, M. Walter and Z. Yang, “Holographic duality from random tensor networks,” JHEP **1611**, 009 (2016) doi:10.1007/JHEP11(2016)009 [arXiv:1601.01694 [hep-th]].
- [43] C. Akers and P. Rath, “Entanglement Wedge Cross Sections Require Tripartite Entanglement,” JHEP **04**, 208 (2020) doi:10.1007/JHEP04(2020)208 [arXiv:1911.07852 [hep-th]].
- [44] A Hatcher, “Pants Decompositions of Surfaces,” [ arXiv:math/9906084].